

# Blade couple with dry friction connection

L. Půst<sup>a,\*</sup>, L. Pešek<sup>a</sup>, A. Radolfová<sup>a</sup>

<sup>a</sup>*Institute of Thermomechanics, AS CR, v.v.i., Dolejškova 5, 182 00 Prague, Czech Republic*

Received 12 January 2015; received in revised form 22 June 2015

---

## Abstract

Vibration of a blade couple damped by a dry friction contact in the shroud is investigated by means of hysteresis loops and response curves analysis. The studied system is excited by one harmonic external force in a frequency range near to the lowest eigenfrequency of real blades. Blades are connected by means of a damping element consisting of dry friction part linked in series with linear spring. This “stick-slip” damping element is supposed to be either weightless or of a very small mass which models the mass of elastically deformed parts of contacting bodies near the friction surface. Two approximate mathematical models of “stick-slip” dry friction elements are suggested and analysed. The response curves of blade couple connected by stick-slip damping element are presented for different values of slip friction forces and two values of mass of elastically deformed parts.

© 2015 University of West Bohemia. All rights reserved.

*Keywords:* stick-slip dry friction, 3V friction characteristic, tangential contact stiffness, hysteresis loop, response curves

---

## 1. Introduction

Dry friction connections are very often used in technical applications for quenching of dangerous resonance or self-excited vibrations [1–4, 7, 11]. Many theoretical, numerical and experimental investigations of dynamic properties of turbine blades have been done with the aim to develop means for reduction of dangerous resonance amplitudes of blades. The dynamic systems investigated, for example, in papers [5, 6, 8] contain dry friction elements modelled by relatively simple 2V (two variables) “force-velocity” characteristics. Application of these mathematical models enables easy calculation for the majority of engineering problems where the vibrating bodies can be assumed to be stiff and when these bodies in contact surfaces only slip against each other without any elastic deformation. Such models correctly describe the properties of dry friction process for sufficiently large amplitude of relative motion in contact surfaces.

However, in dry friction elements used for vibration damping, these relative amplitudes of friction couples are usually very small. Also the friction surfaces are sometimes placed on relative compliant parts of moving bodies. Therefore in such cases, it is necessary to use more sophisticated 3V computational “stick-slip” model with “force-velocity-displacement” characteristic for computational analyses. A detailed analysis of the influence of rough surfaces on friction properties is given in [12].

A large part of research activities in world literature is oriented on the investigation of dynamics of turbine disk, with blades connected by friction elements in shroud. For the purpose of a detail analysis of friction processes and their influence on blades vibrations, the dynamic tests of a separated blade couple were performed together with parallel theoretical investigations.

---

\*Corresponding author. Tel.: +420 266 053 212, e-mail: pust@it.cas.cz.

Papers [5,6] describe the influence of various mathematical models of dry friction forces on the response curves of harmonically excited blade couple.

The dynamic systems investigated in both these papers contain a friction connection, described by the simplest types of 2V Coulomb dry friction mathematical model and its modified version without any elastic deformation of contacting bodies.

Presented work describes mathematical models of two types of 3V “stick-slip” damping elements with force-velocity-displacement characteristics and provides an analysis of their properties. These non-linear friction elements are used as damping connections between blades. The effects of tangential micro-deformations in contact surfaces as well as dry friction forces and excitation amplitudes on response curves will be shown and discussed.

## 2. Stick-slip contact with elastic micro-deformation

Dry friction characteristics described by 3V “force-velocity-displacement” are necessary to be used in the cases, when the friction surface is placed on some relative compliant parts of moving bodies and when the contacting bodies vibrate with small relative amplitudes. Such situation is shown in Fig. 1. The motion of bodies is usually defined in analytical or numerical solutions by motion  $x_1(t)$  of the centre of gravity, which can be far from the position of friction contact defined as  $x(t)$  in Fig. 1.

The mathematical model of such damping element consists of Coulomb dry friction part consecutively connected to a spring with characteristics

$$\begin{aligned} F_t &= k_t(x - x_1) & \text{if } \dot{x} = 0, & & F_t \in (-F_{t_0}, F_{t_0}), \\ F_t &= F_{t_0} \operatorname{sgn}(\dot{x}) & \text{if } |\dot{x}| > 0, & & F_t = -F_{t_0} \text{ or } F_{t_0}, \end{aligned} \quad (1)$$

where  $F_{t_0}$  is dry friction force at motion. The graphical presentation of this “stick-slip” damping element is given in Fig. 1a–b.

The point A of the spring-damper connection can be supposed either weightless (case shown in Fig. 1a) or with a very small mass  $m_1$  modelling the mass of elastically deformed parts of contacting bodies near the friction surface (case shown in Fig. 1b). In this case, the excitation force  $F_t^*$  is slightly different from  $F_t$  in Fig. 1a.

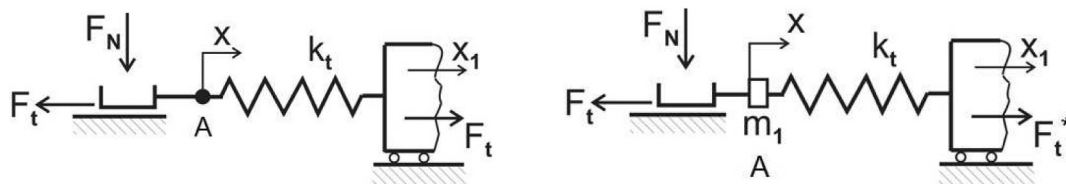


Fig. 1. Two types of stick-slip dry friction models: a) weightless model, b) with small mass  $m_1$

## 3. Hysteresis loops of stick-slip dry friction elements

The hysteresis loop of the weightless “stick-slip” damping element (Fig. 1a) for the simple cosine excitation motion  $x_1(t) = a \cos(\omega t)$  has a rhomboid-form and it contains four break points in one cycle [3, 7]. This exact form is shown in Fig. 2, which is constructed, as well as Figs. 3–4, for dimensions of forces  $F$  in [N], displacements  $x$  and amplitudes  $a$  in [mm] and the stiffness  $k_t$  in [ $\text{kg s}^{-2}$ ].

However, if the relative motion in the contact surface is not so simple (contains higher harmonic components) then the computation is much complicated and it is very inconvenient for

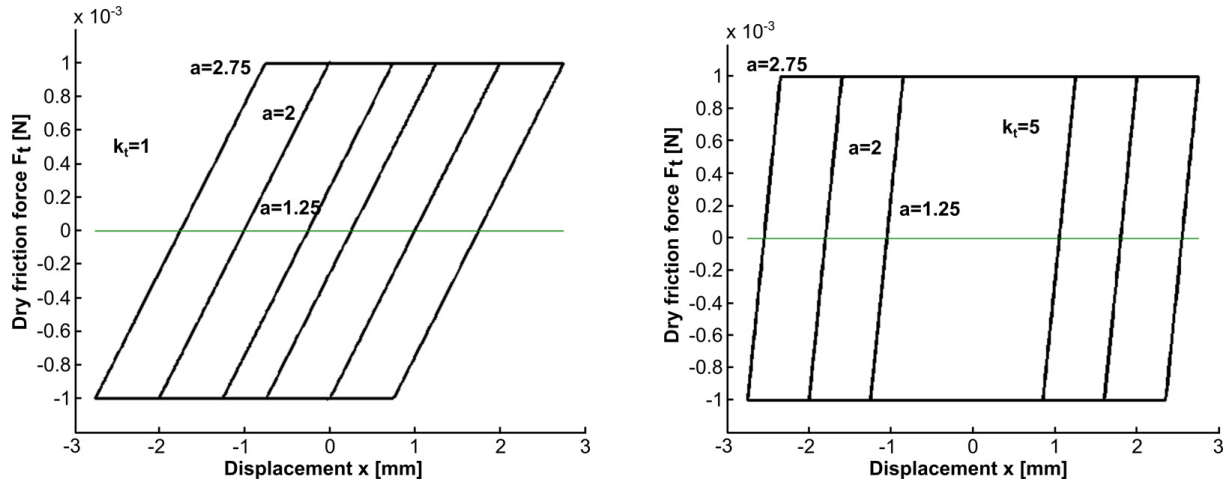


Fig. 2. Exact rhomboid forms

dynamic problems solution. Direct numerical solution (e.g. ODE solvers in Matlab) of ordinary differential equation based on the transformation into a set of first order equations becomes very complex due to the altering function  $sgn$  in friction characteristic. This complication can be removed by expressing the Coulomb law by means of “arc-tangent” function, which is continuous in the whole range of velocity  $\dot{x}$ :

$$F_t = F_{t_0} \frac{2}{\pi} \arctg(\alpha \dot{x}). \quad (2)$$

The parameter  $\alpha$  [s mm<sup>-1</sup>] multiplying the velocity  $\dot{x}$  controls the slope of smooth transition from positive to negative values of friction force in the points of the reversals.

Examples of hysteresis loops with rhomboid-like shape are plotted for three amplitudes  $a = 1.25; 2; 2.75$  mm, for two spring stiffnesses  $k_t = 1$  or  $5$  kg s<sup>-2</sup> and for dry friction element with slip friction force  $F_{t_0} = 10^{-3}$  N in following figures. The equations governing the motions  $x$  of the systems shown in Fig. 1 are

$$k_t(x - a \cos(\omega t)) + F_{t_0} \operatorname{sgn}(\dot{x}) = 0,$$

$$m_1 \ddot{x} + k_t(x - a \cos(\omega t)) + F_{t_0} \operatorname{sgn}(\dot{x}) = 0,$$

where friction forces  $F_{t_0} \operatorname{sgn}(\dot{x})$  can be replaced by equation (2).

The loops of the mathematical mass-less model of the damping element consisting of a spring connected with Coulomb-dry-friction-damper with the “arc-tangent” characteristic (Fig. 1a) are plotted for  $\alpha = 25$  s mm<sup>-1</sup> (see relation 2) in Figs. 3a–b.

The calculation of hysteresis loops for the same parameters but for the mathematical model shown in Fig. 1b, i.e., the model of dry friction stick-slip damping element with a small mass  $m_1 = 0.002$  kg of an elastic deformable part of contacting bodies, gives loops plotted in Figs. 4a–b.

Comparing the results presented in Fig. 2 with those in Fig. 3 and Fig. 4, it is evident that both mathematical models graphically presented in Fig. 1 give very similar properties in the investigated range of parameters both from the point of view of hysteresis loop’s form and area proportional to the friction loss energy. They can be successfully applied for the solution of complicated cases (e.g. at general multi-harmonic excitations) due to the compact definition forms. They are also more advantageous than the stepwise piece-wise solution [3] when one period is divided into several intervals, which are connected together with the ends-beginning conditions.

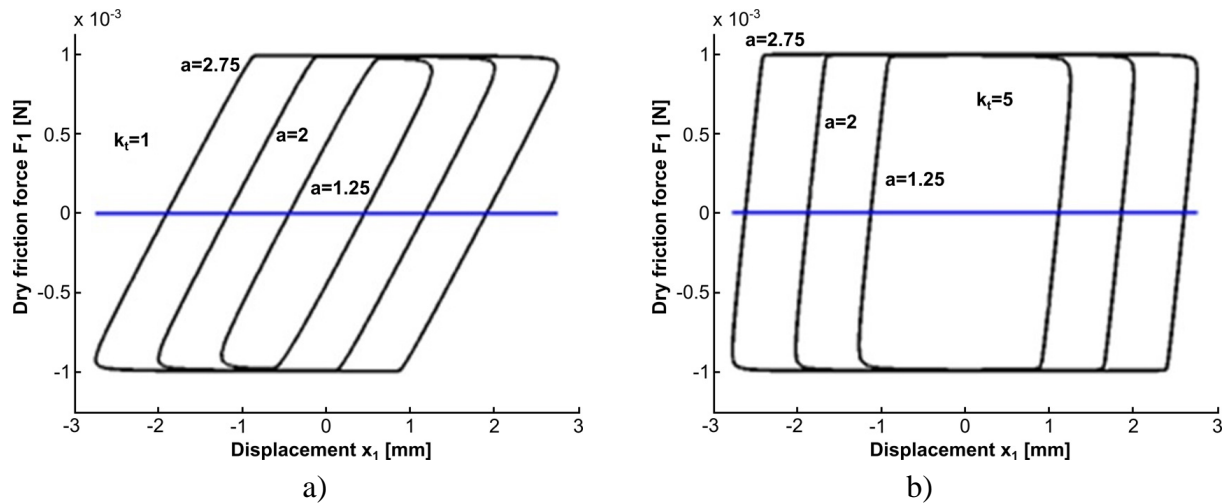


Fig. 3. Hysteresis loops of stick-slip “arc-tangent” friction element for a) weak tangential stiffness  $k_t = 1 \text{ kg s}^{-2}$ , b) strong stiffness  $k_t = 5 \text{ kg s}^{-2}$

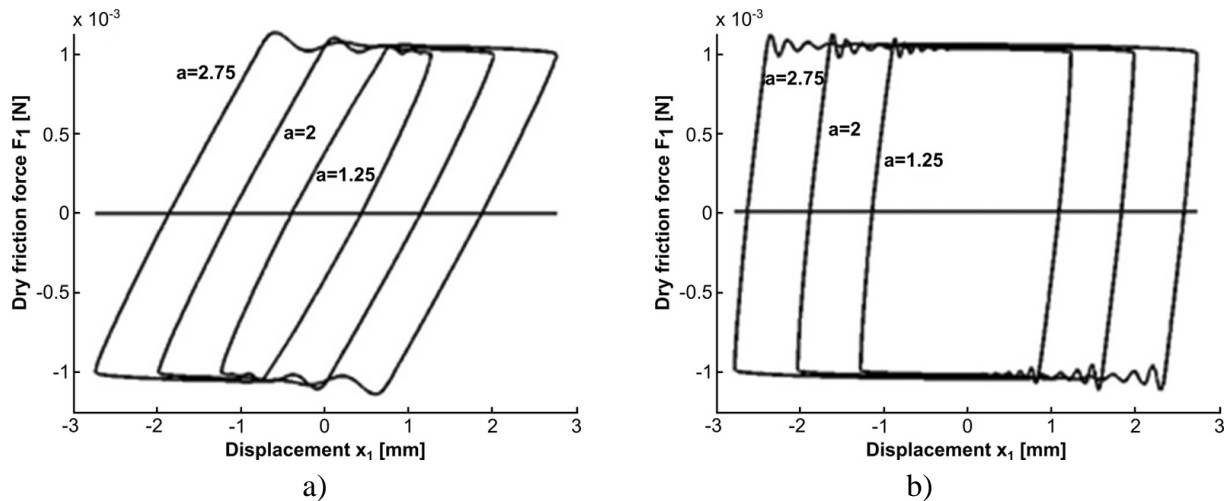


Fig. 4. Hysteresis loops of stick-slip Coulomb dry friction element for a) weak tangential stiffness  $k_t = 1 \text{ kg s}^{-2}$ , b) strong stiffness  $k_t = 5 \text{ kg s}^{-2}$

#### 4. Forced vibration of two-blades bunch with stick-slip damping connections

As it has been mentioned in the section Introduction, a part of research activities is oriented on the investigation of dynamics of turbine disk with blades connected by friction elements in shroud. The gained results of detail analysis of friction processes and their influence on blades vibrations were published in papers [5,6], where the simplest types of 2V Coulomb dry friction mathematical model and its modified version without any elastic deformation of contacting bodies were used.

In this section, the influence of the elastic micro-deformations in the contact surfaces will be analysed using more exact stick-slip friction mathematical models expressed by the 3V force-velocity-displacement characteristics. Laboratory experiments on the blades’ models prepared by a turbine producer were the main motivation for this analysis. The scheme of one of these laboratory models is shown in Fig. 5a. The contact pressure on friction surfaces A was realized either by a spring, or by the torsion pre-stress applied to the oblique cut of shrouding.

The first simplified mathematical model of the blade couple shown in Fig. 5b consists of two identical 1 DOF slightly damped subsystems with the stiffness  $k$  and the damping coefficient  $b$ ,

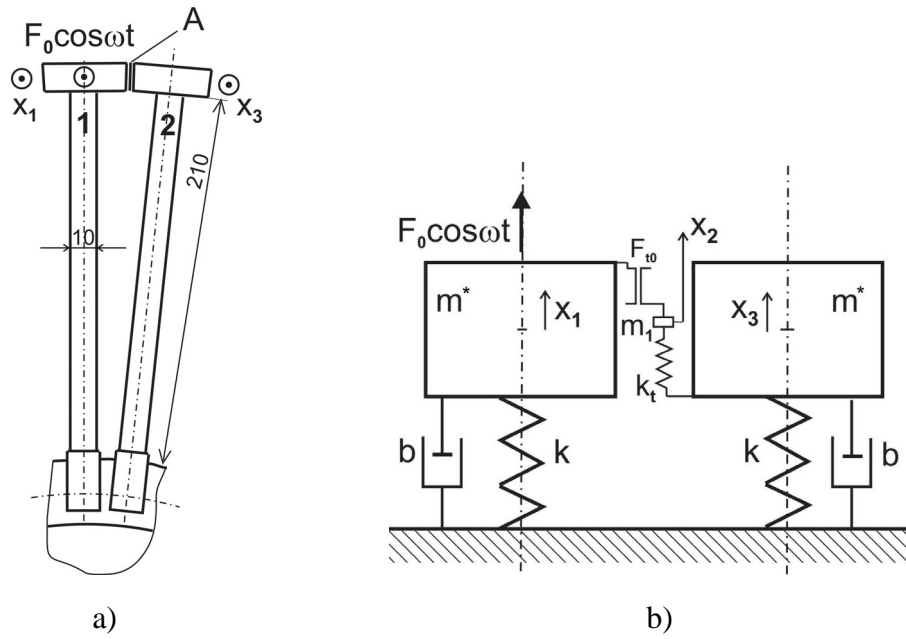


Fig. 5. Two-blades bunch with stick-slip dry friction connection: a) laboratory model, b) mathematical model

roughly corresponding to the experimentally ascertained values of real blades. The modelling of blades dynamic properties by 1 DOF subsystems is possible if the investigation is limited to the lowest resonance frequency range. Between these two subsystems is a small sprig-mass-friction system modelling stick-slip friction element.

Differential equations of motion of such a system with stick-slip dry friction contact, where due to computational reasons an arctg characteristic is applied, are:

$$\begin{aligned} m^* \ddot{x}_1 + b\dot{x}_1 + kx_1 + F_{t_0} \frac{2}{\pi} \operatorname{arctg}[\alpha(\dot{x}_1 - \dot{x}_2)] &= F_0 \cos \omega t, \\ m_1 \ddot{x}_2 + k_t(x_2 - x_3) + F_{t_0} \frac{2}{\pi} \operatorname{arctg}[\alpha(\dot{x}_2 - \dot{x}_1)] &= 0, \\ m^* \ddot{x}_3 + b\dot{x}_3 + kx_3 - k_t(x_2 - x_3) &= 0. \end{aligned} \quad (3)$$

Let the mass of a single blade be  $m$ . The mass  $m_1$  of the elastically deformed part near the contact surface belongs to the blade's mass  $m$ , but during vibrations it moves separately, it is covered by own equation and therefore the masses of blades must be modelled by  $m^* = m - m_1/2$  in the differential equations of motion.

In order to be ready for numerical solution, the equations (3) need to be rearranged into a set of equations of the first order:

$$\begin{aligned} \dot{x}_1 &= v_1, \\ \dot{v}_1 &= (-bv_1 - kx_1 - F_{t_0} \frac{2}{\pi} \operatorname{arctg}[\alpha(v_1 - v_2)] + F_0 \cos \omega t) / (m - m_1/2), \\ \dot{x}_2 &= v_2, \\ \dot{v}_2 &= \{-k_t(x_2 - x_3) + F_{t_0} \frac{2}{\pi} \operatorname{arctg}[\alpha(v_1 - v_2)]\} / m_1, \\ \dot{x}_3 &= v_3, \\ \dot{v}_3 &= [-bv_3 - kx_3 - k_t(x_3 - x_2)] / (m - m_1/2). \end{aligned} \quad (4)$$

The influence of the dry friction force  $F_{t_0}$  at constant contact stiffness  $k_t = 10\,000 \text{ kg s}^{-2}$  on response curves of both bodies is shown in Fig. 6 for the excitation amplitude  $F_0 = 10 \text{ N}$ , and for four magnitudes of dry friction contact with the slipping force  $F_{t_0} = 2; 4; 6; 8 \text{ N}$ .

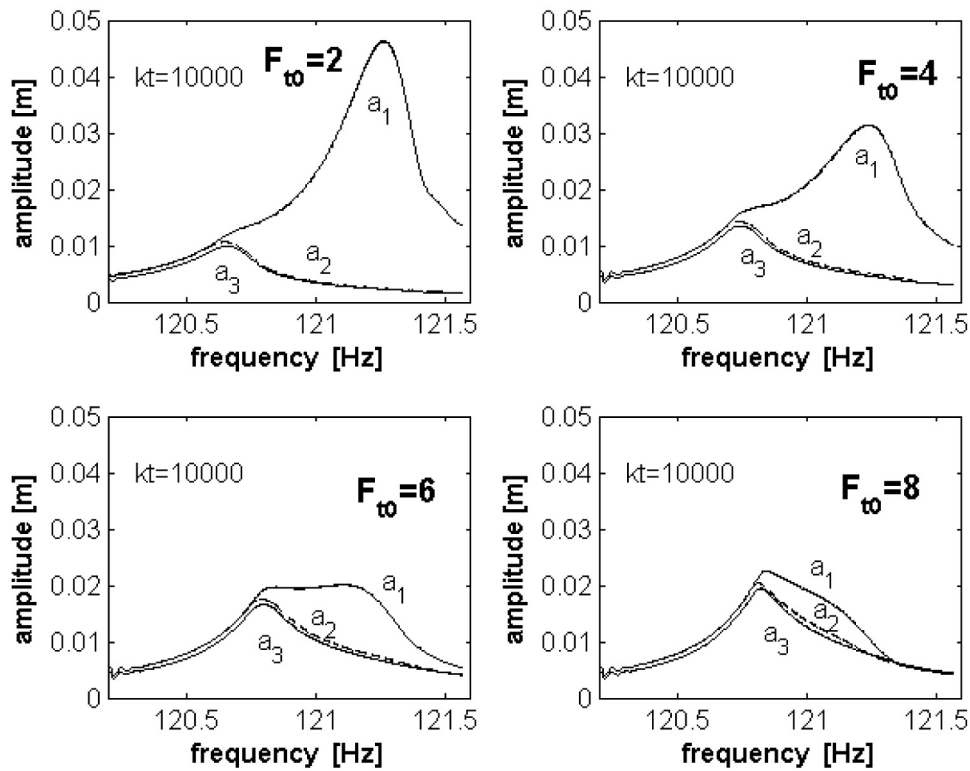


Fig. 6. Response curves of the blade couple model connected by stick-slip damping element. Mass of elastically deformed parts:  $m_1 = m/100$

The function  $\arctg$  was used for the description of the dependence of dry friction force  $F_{t_0}$  on relative slipping velocity  $v = \dot{x}_2 - \dot{x}_1$  between the bodies with masses  $m, m_1$ , with sufficiently great parameter  $\alpha = 25 \text{ [s mm}^{-1}\text{]}$  guaranteeing appropriate similarity to the exact Coulomb dry friction characteristic. The small body  $m_1$ , modelling the mass of elastically deformed parts of contacting bodies, is chosen relatively large in order to see its effect on the response curves:  $m_1 = m/100 = 0.00182 \text{ kg}$ . Also the excitation amplitude  $F_0 = 10 \text{ N}$  has been selected sufficiently high in these examples for similar reasons. For ten times lower forces (excitation, elastic, friction, etc.), the amplitudes reduce as well, but the character of the responses remain similar.

There are two response peaks, at the frequencies  $f_r = 121.25 \text{ Hz}$  and  $f_r = 120.75 \text{ Hz}$ . The first one corresponds to the eigenfrequency of the first excited body with mass  $m - m_1/2$ , the second one is given by connected bodies  $m + m_1/2$ . The stiffness  $k_t$  influences the difference between response curves  $a_2(f_r)$  of the small middle body  $m_1$  and  $a_3(f_r)$  of the non-excited body with mass  $m + m_1/2$ . As the stiffness  $k_t = 10\,000 \text{ kg s}^{-2}$  is very high in this case, both curves (the dashed and the solid lower one) lie near each other.

It is evident that the increasing value of the dry friction slipping force  $F_{t_0}$  causes a decrease of amplitudes  $a_1$  of the excited blades to the values of amplitude  $a_2$  which corresponds to the small body  $m_1$  (dashed line). The peaks of these dashed lines together with the peaks of the lower response curves increase with higher dry friction slipping force  $F_{t_0}$ . For the highest friction force  $F_{t_0} = 8 \text{ N}$  (Fig. 6), they overlap with the peak of curve  $a_1(f_r)$  and the investigated system vibrates approximately with very similar amplitudes in the entire frequency resonance range.

If the elastically deformed parts of bodies near the contacting surfaces are twice smaller  $m_1 = m/200$ , then the response curves change. Again, there exist two response peaks, one at

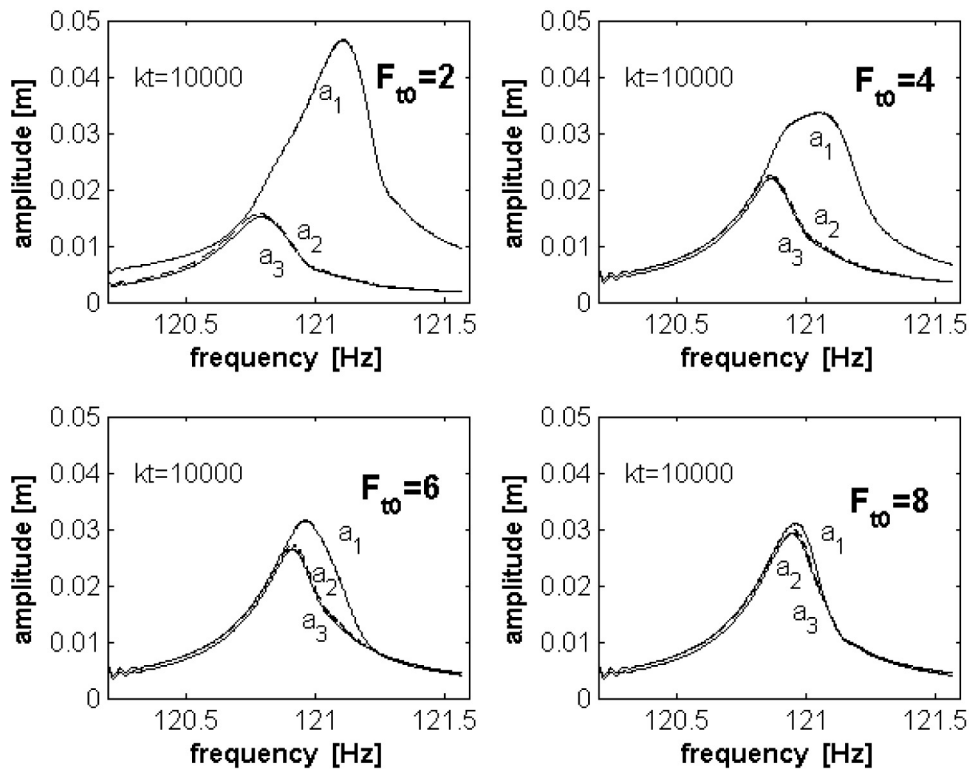


Fig. 7. Response curves of the blade couple model connected by stick-slip damping element. Mass of elastically deformed parts:  $m_1 = m/200$

the response curve  $a_1(f_r)$  of the excited body of mass  $m - m_1/2$  and the second one of the closely joined bodies with response curves  $a_2(f_r)$  and  $a_3(f_r)$ . Due to the smaller body mass  $m_1$ , the frequency difference between these peaks is smaller than in the previous case. The maximum amplitude  $a_1$  of the excited body decreases with increasing dry friction force  $F_{t_0}$ , but the maximum of amplitudes  $a_2, a_3$  increase simultaneously. All curves form a narrow bunch of response curves at the highest friction force  $F_{t_0} = 8$  N.

The results of the numerical solution presented in Fig. 6 and Fig. 7 seem not to be realistic, as the gained amplitudes of vibrations up to 5 cm cannot occur in a real turbine. These high values are caused by the application of a large excitation force of the amplitude  $F_0 = 10$  N acting on the relative small blade used by laboratory experiments ( $m = 0.182$  kg). In order to show that these illustrative results can be successfully applied also to an analysis of real blade's responses, the next figure presented the results calculated for ten times lower excitation and for ten times lower friction forces ( $F_0 = 1$  N,  $F_{t_0} = 0.2; 0.4; 0.6; 0.8$  N) is added.

From the comparison of Fig. 6 and Fig. 8 it is evident that the qualitative properties of blade's responses are valid also for vibration with small amplitudes, of course when the conditions of physical similarity such as the ratio of forces  $F_0/F_{t_0}$  are fulfilled. The measurements of physical model of a blade couple (e.g. [9]) confirm the main properties of responses on harmonic excitations as well as that the form of hysteresis loops can be modelled by the stick-slip friction elements.

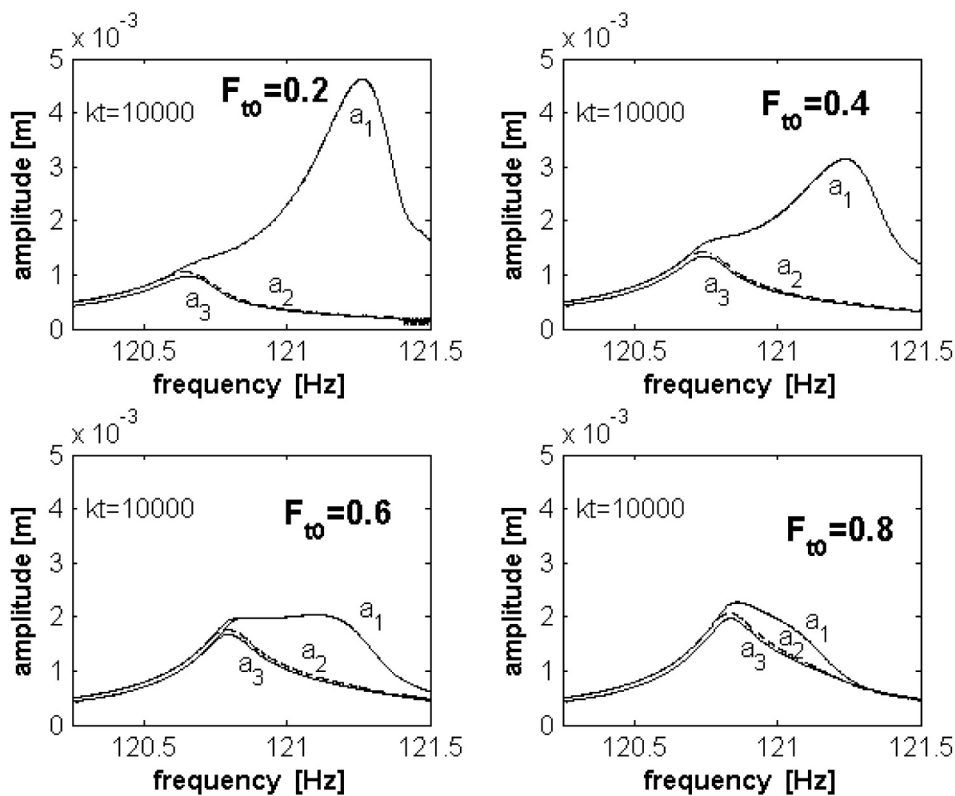


Fig. 8. Response curves of the blade couple model connected by stick-slip damping element. Mass of elastically deformed parts:  $m_1 = m/100$ , amplitude of excitation  $F_0 = 1$  N

### 5. Symmetrical slip-stick friction element

The frequency shift between the peaks of response curves  $a_1(f)$ ,  $a_2(f)$  in Figs. 6–8 are caused by the non-symmetry of the slip-stick friction element connected with a spring to the body 1 and with a dry friction contact to the body 2. This frequency shift can be removed by the application of a more exact slip-stick friction connection consisting of two springs and two mass bodies between which a dry friction element is placed — see Fig. 9.

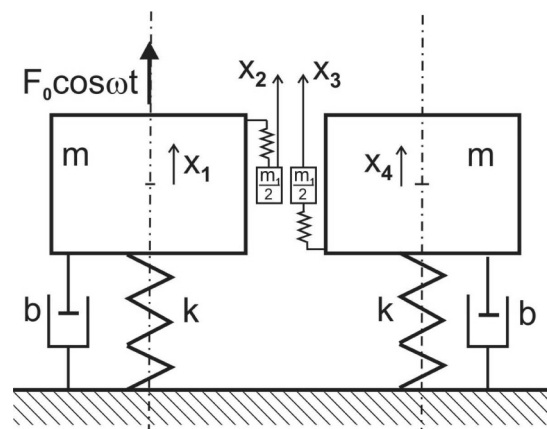


Fig. 9. Model of two-blades bunch with symmetrical stick-slip dry friction connection

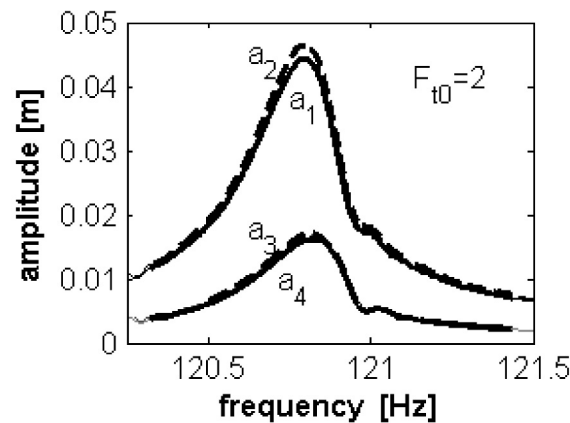


Fig. 10. Response curves of the blade couple model with symmetrical stick-slip damping elements

An example of response curves for the same parameters as used in Fig. 6 is presented in Fig. 10.

Comparing the last figure with the first subfigure in Fig. 6 it is obvious that the blade couple connected by the symmetric slip-stick friction element has the same resonant frequencies of both main bodies and that the peak amplitudes of response curves with the symmetric and non-symmetric friction elements are similar. It can be estimated that the courses of responses in both cases are different, but the damping effect of symmetric and non-symmetric structure are approximately the same.

The symmetrical model is applicable for modelling of a steel–steel friction contact. The non-symmetric model of slip-stick friction elements can be used when the contacting surfaces have different properties. Such cases were investigated, for example, in reports [9, 10], where various combinations of friction couples used in praxis were studied.

## 6. Conclusion

Two main types of stick-slip mathematical models with 3V “force-velocity-displacement” characteristics are presented and analysed by means of hysteresis loops at the harmonic excitation. It is shown that the approximate models with *arctg* description of Coulomb dry friction law as well as models including the inertia of elastically deformed parts near the contact surfaces have very similar rhomboid hysteresis loops as the exact piecewise solution.

The response curves of two-blades bunch with internal connection of blades by means of damping element with the inertia stick-slip characteristic and *arctg* description of dry friction have been investigated. The analysis of influence of different dry friction force and two values of elastically deformable parts near the contact surface on response curves showed the existence of two resonance peaks. Their heights and positions strongly depend on all parameters of 3V characteristic of connecting element. This frequency shift between the resonance peaks can be removed by the application of a more exact slip-stick friction connection consisting of two springs and two mass bodies between which a dry friction element is placed.

## Acknowledgements

The work has been supported by the conceptual development fund RVO: 61388998 of the Institute of Thermomechanics AS CR, v.v.i.

## Reference

- [1] Brůha, J., Zeman, V., Vibration of bladed disk with friction elements, Proceedings of the conference Dynamics of Machines 2014, Prague, IT AS CR, 2014, pp. 15–22.
- [2] Byrtus, M., Hajžman, M., Zeman, V., Linearization of friction effects in vibration of two rotating blades, Applied and Computational Mechanics 7 (1) (2013) 5–22.
- [3] Ding, Q., Chen, Y., Analyzing resonance response of a system with dry friction damper using an analytical method, Journal of Vibration and Control 14 (8) (2008) 1 111–1 123.
- [4] Pfeifer, F., Hájek, M., Stick-slip motion of turbine blade dampers, Philosophical Transactions of the Royal Society of London, Series A338 (1651) (1992) 503–517.
- [5] Půst, L., Pešek, L., Influence of delayed excitation on vibrations of turbine blades couple, Applied and Computational Mechanics 7 (1) (2013) 39–52.
- [6] Půst, L., Pešek, L., Vibration damping by dry friction with micro-slips, Proceedings of the conference Dynamics of Machines 2013, Prague, IT AS CR, 2013, pp. 93–102.
- [7] Půst, L., Pešek, L., Radolfová, A., Various type of dry friction characteristics for vibration damping, Engineering Mechanics 18 (3-4) (2011) 203–224.
- [8] Půst, L., Pešek, L., Radolfová, A., Vibrations of blades couple connected by slip-stick dry friction, Proceedings of the 30th conference Computational Mechanics, University of West Bohemia, Špičák, 2014, pp. 117–118.
- [9] Půst, L., Veselý, J., Horáček, J., Radolfová, A., Effect of friction forces on dynamics of blades' model, Report Z-1412/07, IT ASCR, 2007, (in Czech).
- [10] Půst, L., Veselý, J., Horáček, J., Radolfová, A., Investigation of friction effects on blades' model, Report Z-1422/10, IT ASCR, 2010, (in Czech).
- [11] Sextro, W., Dynamical contact problems with friction, Springer-Verlag Berlin Heidelberg, 2007.
- [12] Voldřich, J., Modelling of the three-dimensional friction contact of vibrating elastic bodies with rough sur-faces, Applied and Computational Mechanics 3 (1) (2009) 241–252.